Aging-Driven Decomposition in Zolpidem Hemitartrate Hemihydrate and the Single-Crystal Structure of Its Decomposition Products

DANIEL R. VEGA,[1,2] RICARDO BAGGIO,[1] MARIANA ROCA,[3] DORA TOMBARI[3]

[1]Grupo Materia Condensada, GIyA, GAIyANN, CAC, Comisión Nacional de Energía Atómica, Av. Gral. Paz 1499, (1650) San Martín, Buenos Aires, Argentina

[2]Escuela de Ciencia y Tecnología, Universidad Nacional de San Martín, Buenos Aires, Argentina

[3]API Division, GADOR S.A., Calle 10, (1629) Parque Industrial Pilar, Buenos Aires, Argentina

Received 11 June 2010; accepted 3 September 2010

Published online 1 October 2010 in Wiley Online Library (wileyonlinelibrary.com). DOI 10.1002/jps.22358

ABSTRACT: The "aging-driven" decomposition of zolpidem hemitartrate hemihydrate (form A) has been followed by X-ray powder diffraction (XRPD), and the crystal and molecular structures of the decomposition products studied by single-crystal methods. The process is very similar to the "thermally driven" one, recently described in the literature for form E (Halasz and Dinnebier. 2010. J Pharm Sci 99(2): 871–874), resulting in a two-phase system: the neutral free base (common to both decomposition processes) and, in the present case, a novel zolpidem tartrate monohydrate, unique to the "aging-driven" decomposition. Our room-temperature single-crystal analysis gives for the free base comparable results as the high-temperature XRPD ones already reported by Halasz and Dinnebier: orthorhombic, P*cba*, $a = 9.6360(10)$ Å, $b = 18.2690(5)$ Å, $c = 18.4980(11)$ Å, and $V = 3256.4(4)$ Å^3. The unreported zolpidem tartrate monohydrate instead crystallizes in monoclinic $P2_1$, which, for comparison purposes, we treated in the nonstandard setting $P112_1$ with $a = 20.7582(9)$ Å, $b = 15.2331(5)$ Å, $c = 7.2420(2)$ Å, $\gamma = 90.826(2)^\circ$, and $V = 2289.73(14)$ Å^3. The structure presents two complete moieties in the asymmetric unit ($z = 4$, $z' = 2$). The different phases obtained in both decompositions are readily explained, considering the diverse genesis of both processes. © 2010 Wiley-Liss, Inc. and the American Pharmacists Association J Pharm Sci 100:1377–1386, 2011

Keywords: solid-state stability; polymorphism; crystal structure; thermal analysis; hydrate

INTRODUCTION

Zolpidem [*N*,*N*,6-trimethyl-2-(4-methylphenyl)-imidazo(1,2-a)pyridine-3-acetamide, $C_{19}H_{21}N_3$, Scheme 1a] is a nonbenzodiazepine hypnotic drug with similar effects as those of benzodiazepines, by promoting the presence of a particular inhibitory neurotransmitter (gamma-aminobutyric acid, GABA), through the binding to GABA receptors in a similar way and at the same location as to which benzodiazepines bind.[1] The drug appeared in the scientific medium in the mid-1980s,[1] and it has been promoting sustained research work ever since.[2–4] The molecule, classified as an imidazopyridine, is quite different from the benzodiazepine family (Scheme 1b). Its usual commercial presentation is in the form of an hemitartrate hydrate, of which several polymorphs are known, the most common of which are usually referred to in the literature as form A and an alternative form E.[5] Many stable crystallographic forms of a diversity of zolpidem derivatives have also been described in the literature, among them a full tartrate (hereafter, form II), the free base (form III), a saccharinate, etc. Probably due to the difficulty in obtaining single crystals of the different forms, the latter one is, to our knowledge, the only variant that has been thoroughly described so far by single-crystal methods.[6] For one of the commercial forms, the crystal structure had been very briefly described in Ref. 7, but with no numerical data available as to sustain the description either for checking or comparison purposes. This was the state of the art until very

Correspondence to: Daniel R. Vega (Telephone: +54-11-6772-7107; Fax: +54-11-6772-7121; E-mail: vega@cnea.gov.ar)

Journal of Pharmaceutical Sciences, Vol. 100, 1377–1386 (2011)

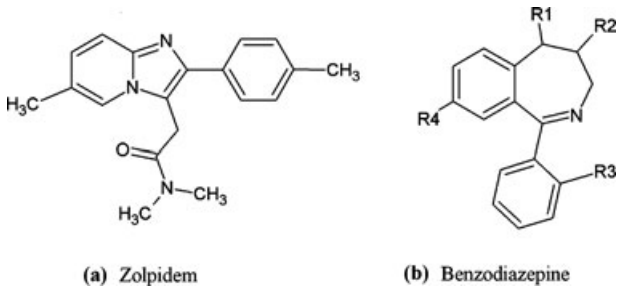

Scheme 1. Structural diagrams of Zolpidem and Benzodiazepine free bases.

recently when Halasz and Dinnebier[4] reported a detailed structural analysis by powder methods of form E of the hemitartrate and two decomposition products identified as the anhydrous 1:1 full tartrate and the free base, referred above as forms II and III, respectively. The products were derived from a "thermally driven" decomposition process and at the same time that the paper provided valuable structural information on crystalline derivatives of zolpidem, it threw light onto a very important aspect of zolpidem hemitartrate thermal decomposition (by the way, a fact not clearly mentioned in Ref. 4), viz. form E suffers on heating the same decomposition process already described for form A in patents WO 00/58310 and US 6242460B1[8] ending up in forms II and III as the final products.

At the time the work by Halasz and Dinnebier[4] appeared, we were engaged in a rather similar project, viz. the single-crystal structural study of some forms of zolpidem tartrate and zolpidem free base (labeled in the present report as IIa and IIIa, scheme 2, to facilitate comparison with structures II and III by Halasz and Dinnebier[4]) as well as their correlation to the products generated in an "aging-driven" decomposition process of form A, which we shall show to be complementary to the already mentioned "thermally driven" one. At this stage, it may be worth mentioning that we could not obtain adequate single crystals for form A, so that the structural study of the starting material could not be performed, as intended.

We shall discuss first the structural results provided by our single-crystal data, then correlate them with the X-ray powder diffraction (XRPD) data of the decomposition products we obtained, and shall leave the comparison with the structural results from powder methods obtained in Ref. 4 and the conclusion derived from this comparison for the final stage of the paper. To make this latter process simpler, we have chosen in our description nonconventional settings of the pertinent space groups, so as to either conform to those used in the Halasz and Dinnebier[4] paper (as in the case of structure IIIa) or to a congruent subgroup (case IIa).

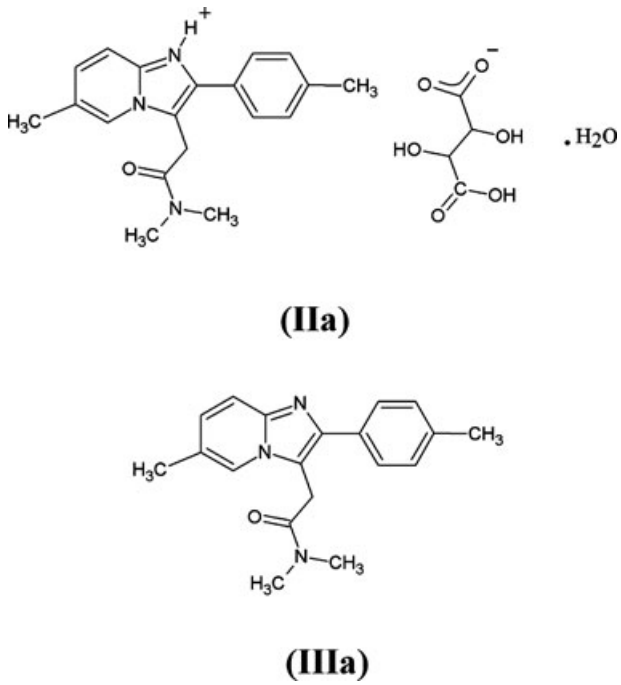

Scheme 2. Structural diagrams of compounds IIa and IIIa.

EXPERIMENT

Powder samples of all three forms, A, IIa, and IIIa were obtained from Gador S.A. (Buenos Aires. Argentine), and used as received for powder diffraction experiments, but conveniently recrystallized from water to obtain single crystals of IIa and IIIa, apt for structural analysis. The X-ray single-crystal data were gathered in a SMART CCD area detector diffractometer (Bruker AXS, Madison, Wisconsin, USA)), using graphite monochromatized Mo-Kα radiation ($\lambda = 0.71069$ Å). Software used for data collection: SMART[9]; for integration and data reduction: SAINT-NT,[9] for absorption correction : SADABS.[9] Measurements were made at room temperature (294K). The structures were primarily solved by direct methods using SHELXS97,[10] and completed (by difference synthesis) and refined (by least squares methods) using SHELXL97.[10] Finally, validation of the models was performed using PLATON.[11] The position of the H atoms attached to O and N was inferred from difference Fourier maps and further idealized (O—H: 0.85 Å, H···H: 1.35, N—H: 0.87 Å); those attached to C were placed at calculated positions (C—H: 0.93 Å; C—H_2: 0.97 Å). On refinement, all of them were finally allowed to ride, with displacement factors $U(H)_{isot} = 1.2/1.5\ U_{host}$. Because of the nonsignificant anomalous scattering effects, Friedel opposites were merged, with what in the case of structure IIa the ratio of the number of observed reflections to the number of refinable parameters became smaller than ideal. In addition, the crystal used for structure IIa showed

 DOI 10.1002/jps

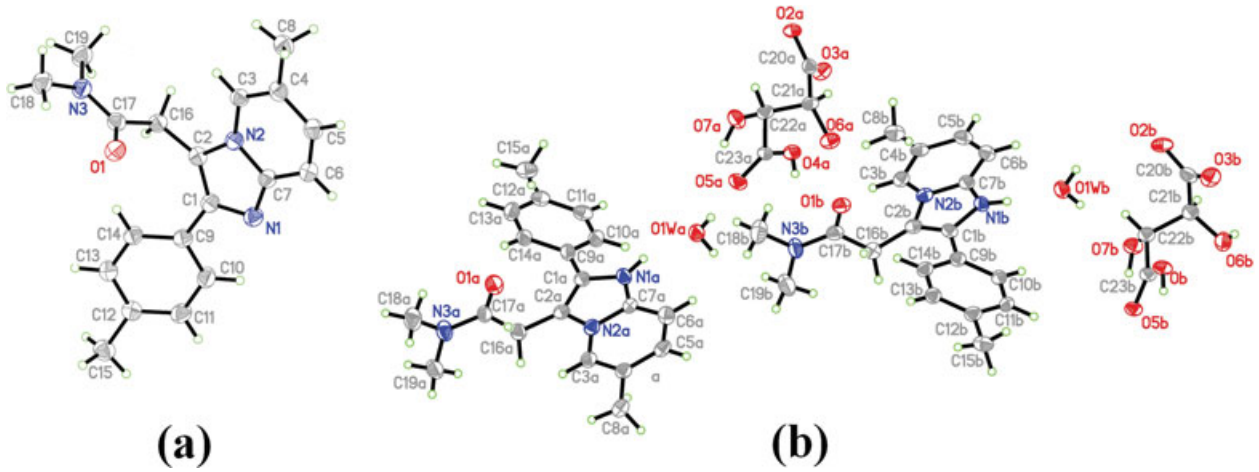

Figure 1. (a) Ellipsoid plot of IIIa, at a 40% probability level. (b) Ellipsoid plot of IIa, at a 30% probability level.

some twinning (monoclinic $\gamma \sim 90^\circ$), which was adequately treated with the SHELXL97[10] instructions "TWIN 1.00 0.00 0.00 0.00 −1.00 0.00 0.00 0.00 −1.00 2" and "BASF 0.13824".

Crystal structure data were deposited in the form of cif files with the Cambridge Crystallographic Data Centre (CCDC) under codes CCDC 768314 and 768315

These data can be obtained free of charge upon request from CCDC via www.ccdc.cam.ac.uk/data_request/cif.

Crystal Structures of IIa and IIIa

Figures 1a and 1b show the corresponding molecular diagrams, and Table 1 shows some relevant crystallographic data for compounds IIIa and IIa. Values in square brackets (when present) display the corresponding values for III and II as provided by the XRPD structural analysis in Halasz and Dinnebier.[4]

The free base (form IIIa) presents one single, unprotonated, zolpidem molecule in the independent unit, whereas form IIa presents two complete independent sets, each one consisting of a protonated

Table 1. Crystal and Refinement Data for IIIa and IIa[a]

Compound	IIIa [III]	IIa [II]
Chemical formula	$C_{19}H_{21}N_3O$ [$C_{19}H_{21}N_3O$]	$C_{19}H_{22}N_3O{\cdot}C_4H_5O_6{\cdot}H_2O$ [$C_{19}H_{22}N_3O{\cdot}C_4H_5O_6$]
Molecular weight	307.39 [307.39]	475.49 [457.51]
Crystal system/Space group	Orthorhombic, P*cab* [Orthorhombic, P*cab*]	Monoclinic, $P112_1$[b] [Orthorhombic, $P2_12_12_1$]
a (Å)	9.6360 (10) [9.9296(4)]	20.7580 (9) [19.9278(8)]
b (Å)	18.2690 (5) [18.4412(9)]	15.2330 (5) [19.9278(8)]
c (Å)	18.4980 (11) [18.6807(9)]	7.2420 (2) [7.6246(2)]
γ (°)		90.123() [90.]
Cell volume (Å^3)	3256.4 (4) [3420.7(3)]	2289.73 (14) [2299.5(2)]
T (K)	294 [413]	294 [413]
Diffraction technique	Single crystal [XRPD]	Single crystal [XRPD]
Z	8	4
μ (mm^{-1})	0.08	0.11
Crystal size (mm)	0.22 × 0.05 × 0.03	0.30 × 0.06 × 0.02
Measured reflections	5311	12808
Independent reflections	2873	4364
Reflections with I > 2σ(I)	1973	3595
R_{int}	0.072	0.108
R[F^2 > 2σ(F^2)]	0.050	0.073
wR(F^2)	0.135	0.202
S	1.02	1.05
Parameters	213	614
$\Delta\rho_{max}$ (e Å^{-3})	0.17	0.40
$\Delta\rho_{min}$(e Å^{-3})	−0.22	−0.33

[a] In square bracket, corresponding values for III and II, respectively.
[b] A nonstandard setting of $P2_1$.

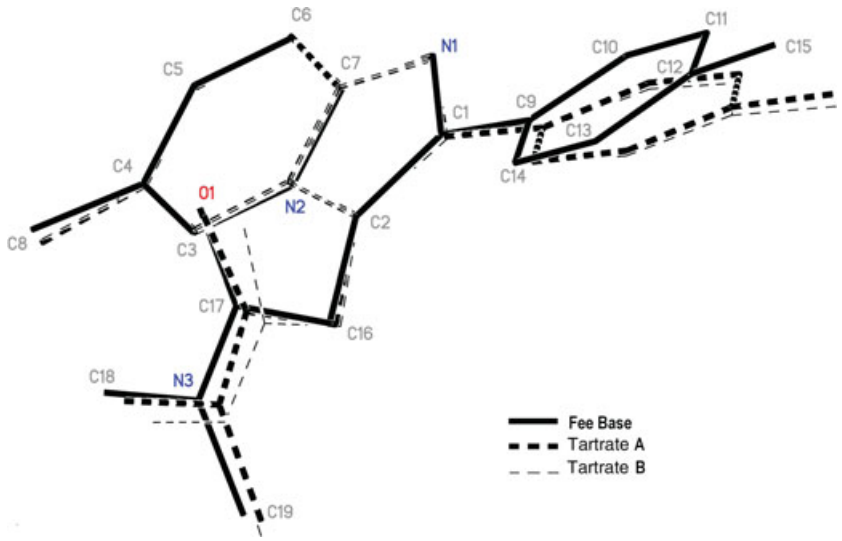

Figure 2. Schematic superposition of the three independent zolpidem moieties.

zolpidem^{+1} cation, a tartrate^{-1} anion, and a hydration water molecule, labeled with trailing letters "a" and "b", respectively. The metrics in the zolpidem unit in both compounds are quite similar and do not reflect any significant difference between forms. In general terms, the molecules also present similar conformations, with only some minor differences in the relative orientation of their planar groups. Both independent zolpidem ions in form IIa appear almost indistinguishable and differ only slightly from the molecule in the free base (Fig. 2) , with the difference residing mainly in the phenyl group region. The two independent moieties in IIa have their six member rings parallel to each other and the (very similar) deviations from the imidazo(1,2-a)pyridine plane [32.2(1)°–33.5(1)°, respectively] are due almost exclusively to a rotation around the C1—C9 bond. That this is so (an almost pure rotation) is evidenced by the nearly perpendicular disposition between the bridging C1—C9 vector and the plane normals [angles subtended: 92.4(1)°, 90.8(1)° in unit "a"; 92.4(1)°, 90.8(1)° in unit "b"]. In the free base, the equivalent angles are a bit larger [94.8(1)°, 94.5(1)°], suggesting an additional out-of-plane bending of the phenyl group.

There are, in addition, some expectable misfits in the very labile acetamide region due to the rotational degrees of freedom associated with the group.

Being the molecules almost identical, the main difference between the free base (IIIa) and the tartrate (IIa) is to be found in the packing configuration and the H-bonding scheme.

The free base crystal structure is featureless, basically governed by weak C—H···O, C—H···N, and C-H···π interactions (Table 2) and π···π interactions (Table 3), which lead to a rather weakly interacting distribution of monomers disposed as undulating chains running along [100] (Fig. 3). The first three contacts in Table 2 and the one in Table 3 provide to the chain formation along [100], whereas the last two in Table 2 serve to link chains along [010] and [001], respectively.

Table 2. Hydrogen-bond Geometry (Å, °) for IIIa

D—H···A	D—H	H···A	D···A	D—H···A
C19—H19B···O1^a	0.96	2.54	3.414(3)	152
C16—H16B···O1^a	0.97	2.60	3.530(3)	162
C19—H19a···Cg1^a	0.96	2.90	3.454(2)	118
C11—H11···O1^b	0.93	2.59	3.497(3)	166
C8—H8B···N1^c	0.96	2.58	3.485(3)	158

Symmetry codes: ^{a}x+1/2, −y+1/2, z; ^{b}−x+1, −y+1/2, z+1/2; ^{c}x+1/2, −y+1, −z+1/2.

Form IIa, instead presents an interesting H-bonded, double-chain strip structure (Table 4 and Fig. 4) made up by two interlinked, very similar chains running along [001], each one embodying as their elemental constituent one of the two independent sets mentioned above, composed of one zolpidem cation, one tartrate anion, and one water solvate, each set characterized by a trailing label "a" or "b" [Fig. 4, where, in order to simplify the view, the zolpidem molecules have been represented by their naked "nuclei", with their two active H-bonding sites (O, N) protruding outwards]. The similarity in both

Table 3. π–π Interactions (Å, °) for IIIa

Group 1/Group 2	ccd (Å)	ipd (Å)	sa (°)
Cg1/Cg2^a	3.8132 (12)	3.42 (18)	25 (3)

Symmetry codes: ^{a}1/2+x,1/2-y,z. Cg1: N1—C1—C2—N2—C7; Cg2: C9—C10—C11—C12—C13—C14 **ccd**, center-to-center distance (Distance between ring centroids).

ipd, mean interplanar distance (Distance from one plane to the neighboring centroid).

sa, mean slippage angle (Angle subtended by the intercentroid vector to the plane normal). For details, see Janiak.[14]

DOI 10.1002/jps

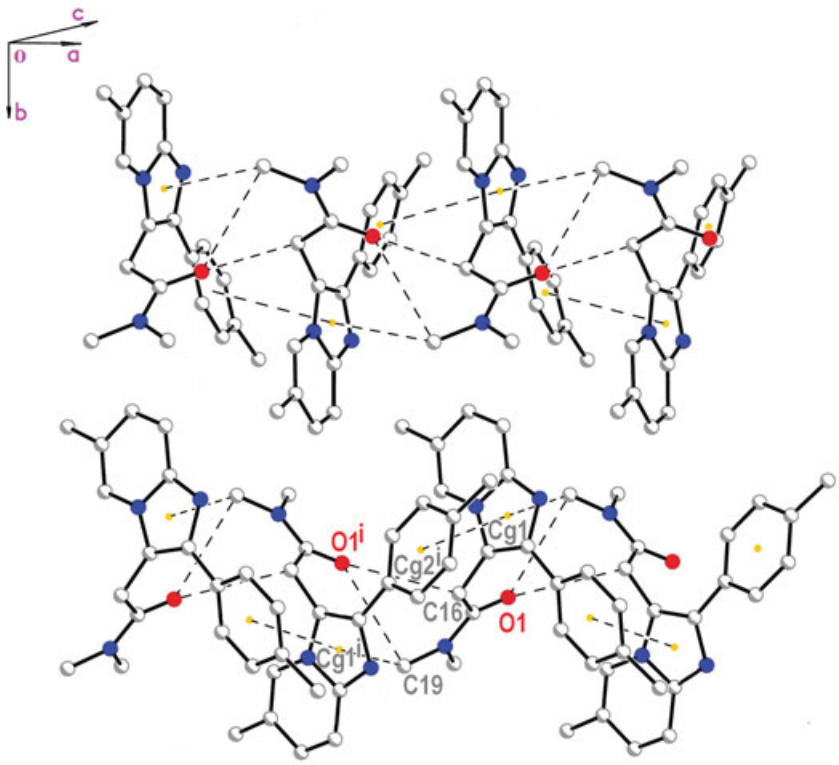

Figure 3. Schematic packing diagram of IIIa showing the undulated chain formed by the weakly interacting Zolpidem free base monomers. Symmetry codes: (i) 1/2 + x, 1/2 − y, z

Table 4. Hydrogen-bond Geometry (Å, °) for IIa

D—H···A	D—H	H···A	D···A	D—H···A
N1A—H1A···O1WA	0.86	1.86	2.689 (8)	161
O4A—H4A···O2A[a]	0.85	1.66	2.507 (6)	180
O6A—H6A···O3A	0.85	2.26	2.711 (7)	113
O7A—H7A···O5A	0.85	2.02	2.581 (7)	122
O1WA—H1WA···O5A	0.85	1.87	2.718 (8)	176
O1WA—H1WB···O7A[a]	0.85	1.97	2.810 (8)	172
N1B—H1B···O1WB	0.86	1.80	2.653 (7)	171
O4B—H4B···O2B[a]	0.82	1.70	2.496 (7)	163
O6B—H6B···O3B	0.85	2.12	2.626 (8)	118
O7B—H7B···O5B	0.85	2.12	2.628 (6)	118
O1WB—H1WD···O7B	0.85	1.87	2.713 (7)	170
O1WB—H1WC···O5B[b]	0.85	1.87	2.717 (7)	176
O6A—H6A···O1B[c]	0.85	2.39	2.860 (7)	116
O7B—H7B···O1B[d]	0.85	2.23	2.962 (7)	144
C3A—H3A···O4B	0.93	2.41	3.296 (9)	159
C5A—H5A···O3B[e]	0.93	2.54	3.457 (9)	170
C10A—H10A···O1A[f]	0.93	2.52	3.120 (10)	122
C14B—H14C···O3A[g]	0.97	2.45	3.408 (9)	171
C14B—H14D···O1WB[d]	0.97	2.52	3.452 (9)	162
C18B—H18D···O4A[h]	0.96	2.38	3.334 (10)	170
C19a—H19c···Cg2[f]	0.96	2.89	3.680 (9)	140
C19b—H19e···Cg6[d]	0.96	2.82	3.677 (9)	149

Symmetry codes: [a] x, y, z+1; [b] x, y, z−1; [c] x−1, y, z; [d] −x+1/2+, −y+2, z+1/2; [e] −x+1/2+, −y+2, z+1/2; [f] −x+1/2+, −y+1, z+1/2; [g] x+1, y, z+1; [h] x+1, y, z.

"a" and "b" parallel arrays is apparent and suggests some kind of frustrated symmetry in the structure. This will be further discussed when comparing with structure II.

Both independent chains are built up around identical $R_3^3(12)$ loops[12] formed by strong O—H···O interactions involving tartrate anions and water molecules, where a strong head-to-tail bond between the former appears as the leading interaction. The lateral interchain connectivity is achieved by "b" type zolpidem cations, which bridge the tartrate–water chains by way of O6a—H6a···O1b, N1b—H1b···O1Wb contacts (Fig. 4 and Table 4). As atom O1a is not involved in conventional H-bonding, type "a" zolpidem cations interact with the rest just through one side, via the N1a—H1a site, and thus only laterally decorate the strips. There are, in addition, some extra and much weaker O—H···O, C—H···O, and C—H···π bonds (Table 4) as well as π···π contacts (Table 5), linking strips together into a three-dimensional H-bonded network.

Zolpidem Hemitartrate Stability

A number of systematic works have confirmed along the years the suspected solid-state instability of the commercial forms of zolpidem hemitartrate, the most important ones being those reported by Lawecka et al.[13] (no specific starting form mentioned in the paper), patent #WO 00/583108 (starting from form A) and Halasz and Dinnebier[4] (starting from form E). In the first one, the authors resorted to a variety of driving agents (aging, heating) and

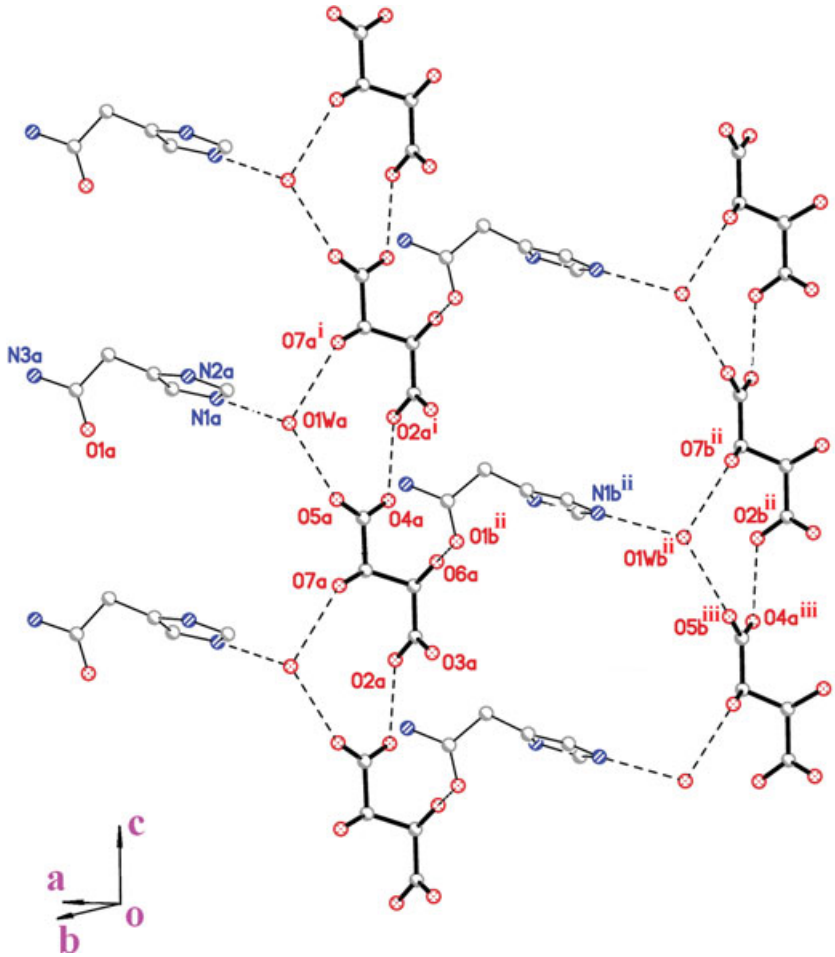

Figure 4. Schematic packing diagram of IIa showing the way a strip is formed. For clarity H atoms were omitted and the Zolpidem units were idealized by their nuclei, with the two H-bonding active sites (O, N—H) present. Symmetry codes: (i) x, y, 1 + z; (ii) −1 + x, y, z; (iii) −1 + x, y, −1 + z.

Table 5. π–π Interactions (Å, °) for IIa

Group 1/Group 2	ccd (Å)	ipd (Å)	sa (°)
Cg1/Cg3[a]	3.657 (4)	3.389 (5)	22.0 (2)
Cg5/Cg7[b]	3.710 (4)	3.338 (3)	25.8 (1)

[a] 1/2-x,1-y,-1/2+z; [b] 3/2-x,2-y,1/2+z. Cg1 N1a—C1a—C2a—N2a—C7a; Cg3 C9a—C10a—C11a—C12a—C13a—C14a; Cg5 N1b—C1b—C2b—N2b—C7b; Cg7 C9b—C10b—C11b—C12b—C13b—C14b **ccd,** center-to-center distance (Distance between ring centroids).

ipd, mean interplanar distance (Distance from one plane to the neighboring centroid).

sa, mean slippage angle (Angle subtended by the intercentroid vector to the plane normal). For details, see Janiak.[14]

characterization techniques [XRPD, thermogravimetric analysis (TGA), differential scanning calorimetry, etc.] but did not provide further identification of the initial or final products; in the remaining ones instead, a single physical agent (heating) was used to achieve decomposition into a binary product (hereafter IV), and irrespective of differences in the starting material, the same phases (II and III) in a 1:1 mixture identified and characterized. In the present work, we evaluated the "aging" behavior of form A of the hemitartrate aiming to identify the eventual resulting products, for what we planned a controlled, long-term stability check on form A. To achieve this in a systematic way, a number of powder samples of form A were left to age for about 15 months under local ambient conditions (temperature range: ~20 ± 3°C, humidity range: ~70 ± 20%) with a periodic XRPD test control performed on a 3-month interval basis. A word of caution is to be raised here: even if for all the tested probes the same type of decomposition seemed to take place, the velocities at which the process occurred are not comparable to the state that after 1 year some of them were fully converted into a final composite system, hereafter IVa (as was the case reported herein), whereas others still appeared to be midway and even presented detectable traces of some undetermined polymorphic forms.

The outcome of the most conclusive of our experiments is presented in Figure 5a, A–D, in which the

 DOI 10.1002/jps

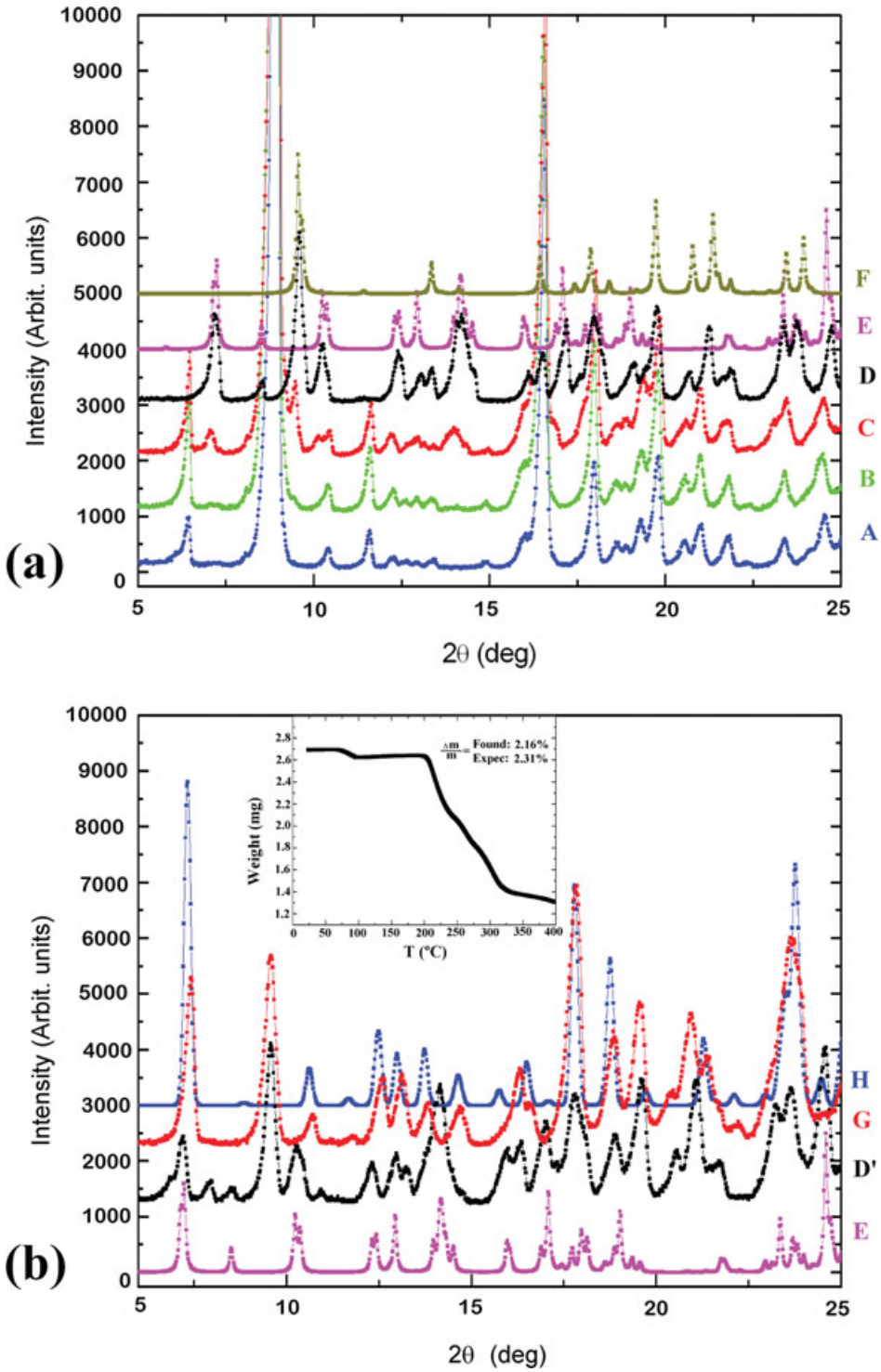

Figure 5. (a) X-ray powder diffraction (XRPD) diagrams of the different forms involved in the decomposition of form A. (A–D): Sequential aging evolution of form A.. (A): fresh sample of form A, (B): after 3 months aging, (C): after 6 months, and (D): after 12 months. (E): Diffraction pattern calculated for compound IIa, (F): diffraction pattern calculated for compound IIIa. The relationship (D) = (E) + (F) is apparent. (b) XRPD of the compounds involved in the thermal dehydration. (E): diffraction pattern calculated for compound IIa, (D′): decomposition product of form A after 2 years aging, (G): sample D′ heated at 100°C, (H): diffraction pattern calculated for compound II.

time evolution of the XRPD diagram of a sample of form A is plotted. Inspection of these diagrams shows that zolpidem hemitartrate hydrate, form A, (Fig. 5a, A) evolves on aging to generate a final composite system IVa (Fig. 5a, D).

The process is rather similar to the one found on heating (Refs. 4 and 8), in that both consist in the segregation of two different zolpidem-containing phases; in the present case, however, the resulting products (readily detectable through their XRPD diagrams) were the full 1:1 tartrate, monohydrate (form IIa; Fig. 5a E), and the free base bearing the unprotonated part (form IIIa; Fig. 5a F). The fact that the former contribution is ascribable to form IIa and not to II, as in the thermally driven decomposition, is apparent from the comparison of the calculated XRPD diagrams for both 1:1 tartrates (Fig. 5b, E and H, respectively); there are many peaks in the final XRPD of the aging decomposition product IVa (Fig. 5a, D), which can be explained by the presence of the former but not by the latter (for instance, the $2\theta \sim 14, 17, 24^\circ$ regions).

To support this assert, we performed what should be a conclusive experiment: the composite decomposition product IVa, as obtained in our experiment the aging process should convert to the final product IV as found in the Halasz and Dinnebier[4] paper by way of a thermal treatment leading to dehydration according to the following equation:

$$\begin{aligned} \text{IVa} = (\text{IIa} + \text{IIIa}) \rightarrow (\text{onheating}) \rightarrow (\text{II} + \text{III}) + \text{H}_2\text{O} \\ = \text{IV} + \text{H}_2\text{O} \end{aligned}$$

This equation presupposes that III (as obtained by thermal decomposition) and IIIa (present paper) are actually one and the same forms of zolpidem free base, a fact that will be thoroughly discussed afterwards; with this in mind, the equation can be written as:

$$\begin{aligned} (\text{Zolp}^{+1}\text{: Tartr}^{-1}\text{: H}_2\text{O}) + (\text{Zolp}^{\circ}) \rightarrow (\text{onheating}) \\ \rightarrow (\text{Zolp}^{+1}\text{: Tartr}^{-1}) + (\text{Zolp}^{\circ}) + (\text{H}_2\text{O}) \end{aligned}$$

Figure 5b shows a sequence showing the experimental outcome: diagram E presents the calculated XRPD diagram of IIa, explaining most of the experimental peaks of the "aging" decomposition product IVa (diagram D', comparable to D in Fig. 5a, even if corresponding to different samples with different decomposition rates). Through a thermal treatment at about 100°C, the resulting product, characterized by the XRPD diagram presented in G, was obtained. This diagram is fully explainable by the peaks in H, corresponding to II.

The insert in Figure 5(b) presents the TGA diagram of this transformation, showing a 75°C –95°C dehydration range and a reasonable agreement for one single water molecule loss in the equation IVa = (IIa : IIIa) → (on heating) → (II : III) + (H_2O) = IV + H_2O.

Mass loss for one H_2O molecule in ($Zolp^{+1}$: $Tartr^{-1}$: H_2O) + ($Zolp^{\circ}$): expected, 2.31%; found: 2.16%.

Comparison of the Present Single-crystal Analysis and the Structural Results Obtained from XRPD

The analogy between both decomposition processes (the one herein reported and the one in Ref. 4) initially suggested that the final composite systems IV and IVa could in principle be the same. On the contrary, a closer inspection of both structural works showed important differences (including metrics, symmetry, and hydration state), which pointed otherwise and merited due analysis. The obvious way to sort this out was to perform a detailed comparison of the results obtained, and to facilitate this job, we "translated" our structural data (space groups, atom positioning in the cell, etc.) into the "language" used in the Halasz and Dinnebier[4] paper.

Comparison of forms III–IIIa was straightforward and provided a definitory test regarding the quality of the powder data results in Ref. 4. Figure 6 presents the plain superposition, without any kind of least squares fitting and just having a common origin for both models of the zolpidem free base. The agreement is more than fair, taking into account cell expansion in form III, solved at 140°C (see Table 1 for details). Both structures superimpose within experimental errors and only differ significantly in some terminal methyl groups, for what the reliability of the XRPD structural work in Ref. 4 was confirmed, thus

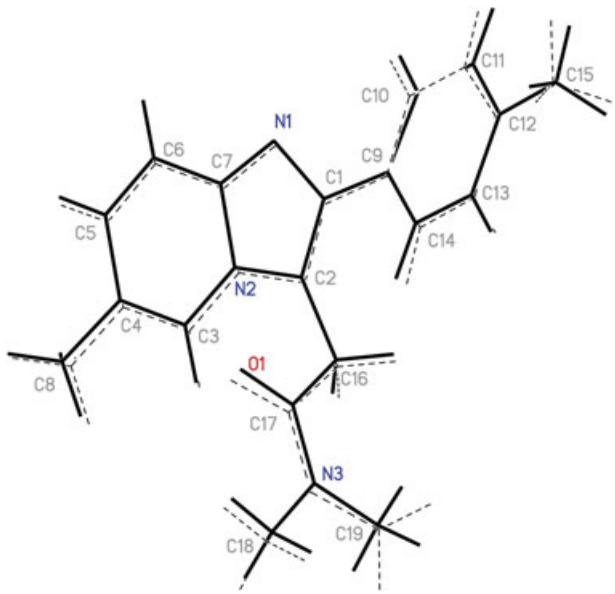

Figure 6. Schematic superposition of the molecular models for structures III (full lines) and IIIa (broken lines), having only fixed origin and cell axis directions.

 DOI 10.1002/jps

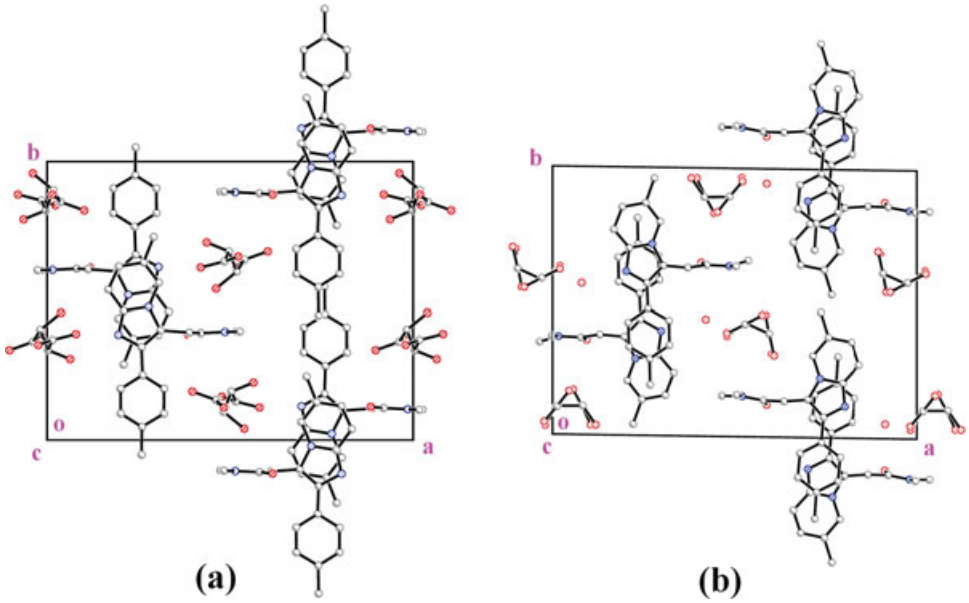

Figure 7. Comparative [001] projections of (a) structures II and (b) IIa.

turning meaningful the more elaborated comparison required for forms II–IIa.

In spite of the many gross structural features shared by forms II–IIa (viz., close similarity in cell metrics, chains of "head-to-tail" H-bonded tartrate anions running along a 2_1 axis, parallel piling of stacked zolpidem molecules "stuffing" the space between chains, etc.), there are a number of details differentiating both structures, and which effects are readily observable, as already stated, in the quite dissimilar calculated XRPD diagrams shown in Figure 5b, diagrams E and H. These differences included metrics (even if similar, the cell constants showed a marked anisotropic variation), composition (the refinement results showed IIa to be a monohydrate, whereas II had been refined as anhydrous, and the unwitting "missing" of one solvent water molecule is hardly reconcilable with high quality Rietveld refinements as obtained in Ref. 4 for structure II), space group ($P112_1$ vs. $P2_12_12_1$; same comment applies), plus a number of finer structural details easily seen in the [001] projections shown in Figure 7. The most obvious is the relative disposition of the zolpidem moieties in the stacking, which in II appears overlapping the fused imidazo–pyridine groups, whereas the corresponding interactions in IIa involve the fused rings of one moiety and the methylphenyl ring of a neighboring one. Also the tartarte moieties exhibit significant internal differences, the planar carboxylate groups being almost parallel in the independent unit in II [dihedral angle: 9.5(1)°], whereas the corresponding values in IIa are 72.1(1)° and 66.4(1)° for units "a", "b", respectively.

Thus, the final conclusion is that decomposition products II and IIa are really different solvatomorphs, even though closely related, and this closeness can include symmetry considerations; as already described for IIa, the structure is characterized by some kind of frustrated symmetry leading to two independent moieties, labeled "a" and "b", in the asymmetric unit (S.G. $P112_1$, $z = 4$, $z' = 2$). The loss of the hydration water molecule seems to provoke a slight, though important, structural rearrangement resulting in a "symmetry upgrade" from a monoclinic S.G. with a (nonconventional) unique angle $\gamma \sim 90°$ toward an orthorhombic supergroup ($P2_12_12_1$, $z = 4$, $z' = 1$, $\gamma = 90°$) having the monoclinic one ($P112_1$) as a subgroup. In this process, the frustrated symmetry leading to two independent (though pseudo-symmetry related) moieties in the asymmetric unit ($z' = 2$) relaxes into a proper symmetry linking both, now with $z' = 1$.

The analysis of the different decomposition processes so far reported for zolpidem hemitartrate encourages the speculation that the highly energetic "thermally driven" process might lead systematically to the same decomposition products (II and III) irrespective of the starting phase (a word of caution at this point is in force; this has been shown only for two of the forms A and E; there are several other forms reported, not subject so far to this kind of analysis); the much milder "aging-driven" process, instead, leads to a different full tartrate, IIa, instead of II.

If the diverse genesis of the two different decomposition processes is taken into account, the diversity of phases observed appears fairly understandable: in the thermally driven → II + III process, the sample of E affords decomposition "during" or "after" dehydration and so cannot but lead to two anhydrous forms. The A → IIa + IIIa process, instead, being performed at room temperature can preserve the overall

hydration contents to the state that the decomposition can be equated (on a unit-cell-basis balance) as:

$$\begin{aligned} A &= (\text{Zolpiden}^{0}\text{: Zolpiden}^{+1}\text{: tartrate}^{-1}\text{: } H_2O) \\ &\rightarrow (\text{Zolpiden}^{+1}\text{: Tartrate}^{-1}\text{: } H_2O) + (\text{Zolpiden}^{\circ}) \\ &= \text{IIa} + \text{IIIa} \end{aligned}$$

In addition, this gives some indirect support to the original hypothesis put forward by George et al.[7] about the coexistence in their hemitartrate of a charged zolpidem moiety plus an unprotonated one, a hypothesis, which could not be confidently confirmed by direct evidence neither at the time of their original work nor in the recent 2010 one by Halasz and Dinnebier.[4]

ACKNOWLEDGMENTS

Powder samples of the three forms A, IIa, and IIIa were provided by GADOR, S.A (Buenos Aires, Argentina). We acknowledge the Spanish Research Council (CSIC) for providing us with a free-of-charge license to the CSD system[15] as well as Facundo Gilles and Daniel Fernández for their help in HT-XRPD and single-crystal-XRPD experiments.

REFERENCES

1. Arbilla S, Depoortere H, George P, Langer SZ. 1985. Pharmacological profile of the imidazopyridine zolpidem at benzodiazepine receptors and electrocorticogram in rat. Naunyn Schmiedebergs Arch Pharmacol 330(3):248–251.
2. Debruyne D, Lacotte J, De HuraultLigny B, Moulin M. 1991. Determination of zolpidem and zopiclone in serum by capillary column gas chromatography. J Pharm Sci 80(1):71–74.
3. Trapani G, Latrofa A, Franco M, Pantaleo MR, Sanna E, Massa F, Tuveri F, Liso G. 2000. Complexation of zolpidem with 2-hydroxypropyl-β-, methyl-β-, and 2-hydroxypropyl-γ-cyclodextrin: Effect on aqueous solubility, dissolution rate, and ataxic activity in rat. J Pharm Sci 89(11):1443–1451.
4. Halasz I, Dinnebier RE. 2010. Structural and thermal characterization of zolpidem hemitartrate hemihydrate (form E) and its decomposition products by laboratory X-ray powder diffraction. J Pharm Sci 99(2):871–878.
5. Aronhime J, Leonov D. 2006. Zolpidem hemitartrate solvate. Patent EP1541146 B1.
6. Banerjee R, Bhatt PM, Ravindra NV, Desiraju GR. 2005. Solid-state architecture of saccharin salts of some diamines. Cryst Growth Design 5(6):2299–2309.
7. George P, Rossey G, Depoortere H, Mompon B, Allen J, Wick A. 1988. Zolpidem and related compounds: Synthesis, physical properties and structure-activity relationships in Imidazopyridines. In Sleep disorders: A novel experimental and therapeutic approach; Sauvanet JP, Langer SZ, Morselli, Eds. New York: PL. Raven Press Ltd., pp 11–24.
8. Ettema GJB, Lemmens JM, Peters THA, Picha F. 2000. Zolpidem salts, Patent WO00/58310; and Ettema GJB, Lemmens JM, Peters THA, Picha F. 2001. Patent US6242460 B1.
9. Bruker. 2002. SMART-NT V5.624. Data Collection Software; SAINT-NT V6.22a (Including SADABS). Data Reduction Software. Siemens Analytical X-ray Instruments Inc., Madison, Wisconsin.
10. Sheldrick GM. 2008. A short history of SHELX. Acta Cryst. A64, pp 112–122.
11. Spek AL. 2003. Single-crystal structure validation with the program PLATON. J Appl Crystallogr 36:7–13.
12. Bernstein J, Davis RE, Shimoni L, Chang NL. 1995. Patterns in hydrogen bonding: Functionality and graph set analysis in crystals. Angew Chem Int (Ed Eng) 34:1555–1573.
13. Lawecka M, Kosmacińska B., Glice M, Korczak K. 2006. The influence of storage conditions on the polymorphic stability of zolpidem tartrate hydrate. J Therm Anal Calorimetry 83(3):583–585.
14. Janiak C. 2000. A critical account on π stacking in metal complexes with aromatic nitrogen-containing ligands. J Chem Soc Dalton Trans 3885–3898.
15. Allen FH. 2002. The Cambridge structural database: A quarter of a million crystal structures and rising. Acta Cryst B58: 380–388.